

# Short scale heterogeneity in the lowermost mantle: insights from PcP-P and ScS-S data

Hrvoje Tkalčić\*, Barbara Romanowicz

*Berkeley Seismological Laboratory, 207 McCone Hall, University of California, Berkeley, CA 94720, USA*

Received 17 December 2001; received in revised form 5 April 2002; accepted 5 April 2002

## Abstract

We compare lateral variations at the base of the mantle as inferred from a global dataset of PcP-P travel time residuals, measured on broadband records, and existing P and S tomographic velocity models, as well as ScS-S travel time data in some selected regions. In many regions, the PcP-P dataset implies short scale lateral variations that are not resolved by global tomographic models, except under eastern Eurasia, where data and models describe a broad region of fast velocity anomalies across which variations appear to be of thermal origin. In other regions, such as central America and southeastern Africa, correlated short scale lateral variations (several hundred kilometers) are observed in PcP and ScS, implying large but not excessive values for the ratio  $R = \partial \ln V_s / \partial \ln V_p$  ( $\sim 2.5$ ). On the other hand, in at least two instances, in the heart of the African Plume and on the edge of the Pacific Plume, variations in P and S velocities appear to be incompatible, implying strong lateral gradients across compositionally different domains, possibly also involving topography on the core–mantle boundary. One should be cautious in estimating  $R$  at the base of the mantle from global datasets, as different smoothing and sampling of P and S datasets may result in strong biases and meaningless results. © 2002 Elsevier Science B.V. All rights reserved.

*Keywords:* traveltime; velocity; D' layer; core–mantle boundary; PcP-waves; ScS-waves

## 1. Introduction

An important question in global geodynamics is whether the 3D seismic velocity anomalies, as seen in tomographic models of the mantle, are of a thermal or a compositional nature, or a combination of both. While global tomographic S

models consistently show predominance of long wavelength structure at the base of the mantle, and in particular two large slow domains in the central Pacific and under Africa, referred to as 'superplumes' (e.g. [1–5]), seismic evidence for shorter scale heterogeneity at these depths is growing. The existence of strong heterogeneity in the vicinity of the two superplumes has been documented through forward modeling of seismic travel times and waveforms (e.g. [6–9]). Recent studies have also found evidence for locally rapid variations in other areas such as middle America (e.g. [10]).

On the other hand, several studies have com-

\* Corresponding author. Present address: Institute of Geophysics and Planetary Physics, 9500 Gilman Drive, University of California, San Diego, La Jolla, CA 92093-0225, USA.

*E-mail address:* hrvoje@seismo.berkeley.edu (H. Tkalčić).

pared global variations in S and P velocities from tomographic inversions, and some of them found evidence for a strong increase in  $R = \partial \ln V_s / \partial \ln V_p$  near the bottom of the mantle, as well as a possible decorrelation between shear and acoustic velocity variations below 2000 km depth (e.g. [11–16]). Furthermore, while there is evidence for zones of strongly reduced P velocity at the base of the mantle (e.g. [17]), there is no evidence that these are accompanied by a comparable drop in S velocity (e.g. [18]).

Through an inversion of PcP-P and PKP(AB-DF) data, we recently obtained maps of  $D''$  with lateral P velocity variations that show much shorter wavelength features than seen in S tomographic models [19]. Here, we consider PcP-P and ScS-S travel time residuals, and analyze their spatial relationship in several regions which are sampled both by PcP and ScS, in comparison to tomographic maps. We discuss implications of our results for the relative variations in P and S velocities in the lowermost mantle, in particular from the standpoint of  $\partial \ln V_s / \partial \ln V_p$  ratios and their interpretation.

## 2. Data

In this study, we use two types of data: (1) PcP-P and (2) ScS-S differential travel time measurements. Our PcP-P dataset was obtained from measurements on vertical components of mainly broadband, and some short period records. In addition to the initial global PcP-P dataset considered in Tkalčić et al. [19], we measured PcP-P data for specific paths bottoming under Africa. Event parameters from the relocated EHB catalog are used [20]. All measurements are done by aligning P and PcP waveforms. All data with poor signal to noise ratio or with different dominant frequencies of P and PcP are discarded, resulting in a measurement precision of  $\sim 0.2$ – $0.5$  s. The differential travel time residuals are then computed with respect to the spherically symmetric reference model *ak135* [21] and corrected for Earth's ellipticity.

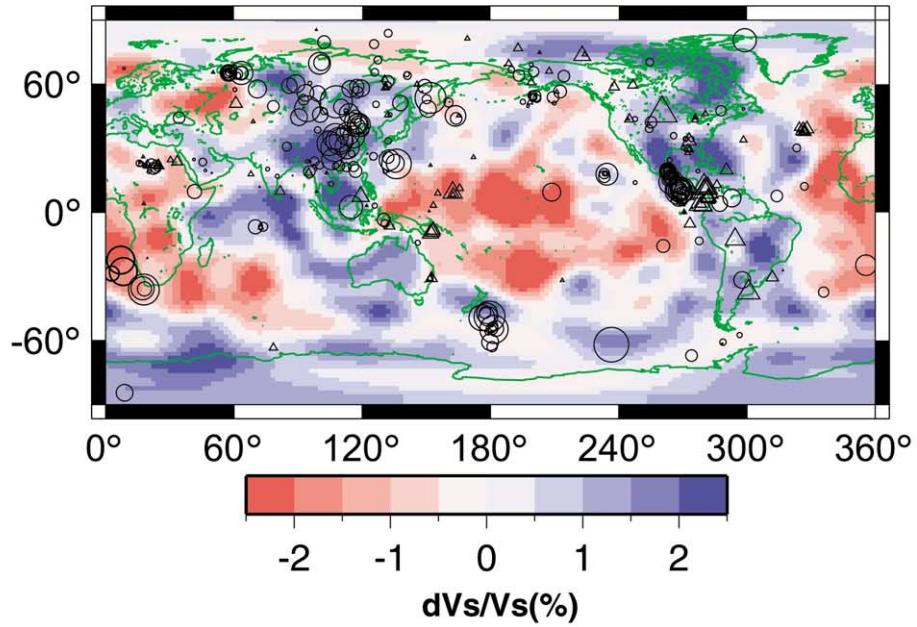
ScS-S differential travel times are measured in the same way as PcP-P, on transverse components

of broadband records, to minimize the contribution from SKS phases. The uncertainty in these measurements is between 0.5 and 1.0 s. We choose ScS-S data so that the coverage of ScS is similar to PcP in the  $D''$  region (hereafter defined as a 300 km thick layer at the base of the mantle) in the specific areas we considered. We also use ScS-S data from the MOMA array (Missouri to Massachusetts Temporary Broadband Seismic Array) measured and used previously by Wysession et al. [10]. ScS-S residuals are calculated with respect to the *PREM* model [22], and also corrected for Earth's ellipticity.

## 3. Results

Fig. 1a,b shows the global distribution of PcP-P travel time residuals, plotted at the surface projection of PcP reflection points on the core–mantle boundary (CMB), with an S and a P tomographic model in the background ([3] and [23], respectively). We selected only data corresponding to epicentral distances  $\geq 55^\circ$ , for which paths of P and PcP are similar, except in the lowermost mantle, so that the travel time residuals should be most sensitive to the structure in the lowermost mantle. The complete dataset has been shown previously in [19]. The spatial coverage of PcP in the lowermost mantle is limited by the available source–receiver geometry. Interestingly, the residuals exhibit a relatively high level of spatial coherence. For instance, a broad area under eastern Asia is well sampled, and there is a consistency in the sign of residuals. Assuming that PcP-P residuals are most sensitive to the structure in the lowermost mantle, their negative sign under eastern Asia is in agreement with a fast anomaly in the lowermost mantle, as seen in most P and S tomographic models (e.g. Fig. 1a,b). On the global scale, most PcP reflection points correspond to fast regions at the bottom of the mantle in the tomographic models. However, not all of them have negative PcP-P residuals, and there are regions with smaller scale lateral variations than indicated by tomographic maps, which deserve more detailed investigation, as will be discussed below.

a)



b)

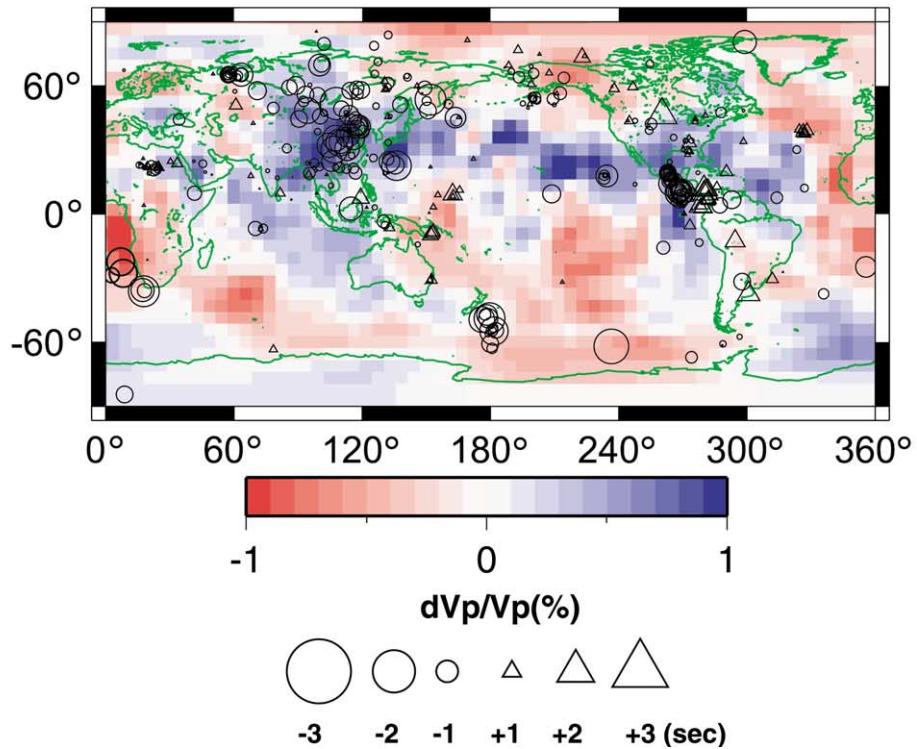


Fig. 1. PcP-P travel time residuals plotted at the surface projections of PcP bouncing points. Residuals are calculated with respect to the *ak135* model, and corrected for ellipticity. Triangles and circles indicate positive and negative residuals, respectively. The background models are: (a) S velocity model *SAW24B16* by [3]; (b) P velocity model by [23].

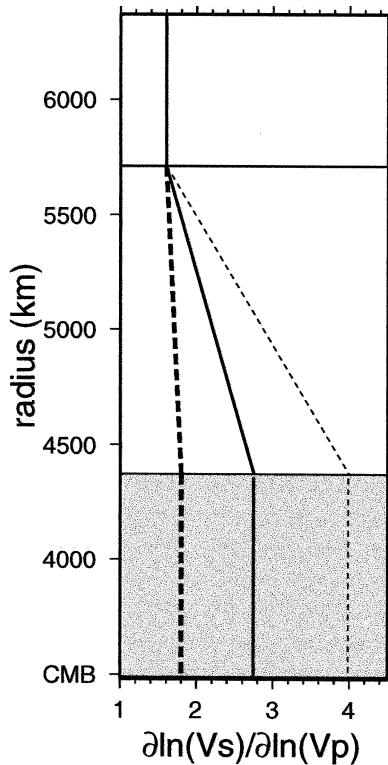


Fig. 2. Best fitting depth profiles of  $R = \partial \ln V_s / \partial \ln V_p$  obtained by comparing PcP-P travel time data to S tomographic velocity models, using a parameter search for the thickness of the bottom layer and the value of  $R$  inside it. Comparison restricted to a subset of PcP-P residuals with PcP reflection points under eastern Eurasia (considered area between 20 and 70°N and 70 and 155°E) with global S tomographic models *SAW24B16* (solid line, variance reduction 57%), and models *SB4L18* and *S362D1* (thick dashed line, variance reduction 60% and 52%, respectively). The thin dashed line corresponds to the best fitting depth profile of  $R$  using the global PcP-P dataset and model *SAW24B16* (variance reduction 10%). Shaded area represents the uncertainty in the thickness of the lowermost layer for the parametrization used.

The apparent consistency of PcP-P residuals and S velocity maps in  $D''$  in eastern Asia gives us the opportunity to try and estimate the ratio  $R$  using a similar approach as in [19], in which we compare observed PcP-P travel time residuals, with those predicted from an existing P tomographic model. Here we do the same, by scaling an existing S tomographic model to P using a given ratio  $R$ , allowing for variations of  $R$  with depth. We performed tests which confirmed that

the PcP-P dataset (for distances  $> 55^\circ$ ) is mostly sensitive to  $R$  in the bottom part of the mantle. We also take into account previous results indicating an increase with depth of  $R$  in the lower mantle (e.g. [11]). We therefore fix  $R = 1.6$  in the upper mantle, allow for a linear increase of  $R$  with depth down to the top of a bottom mantle layer, and a constant  $R$  in that layer. We perform a two parameter search for the thickness of and the value of  $R$  in that layer. Results for three different S models are shown in Fig. 2. The variance reduction for the best fitting  $R$  profile is on the order of 55–60%, depending on the S model considered, and the range of  $R$  obtained at the bottom of the mantle is 1.8–2.7. Variance reduction in PcP-P data is not sensitive to the thickness of the lowermost layer, so we present the results for the best fitting depth profile of  $R$  by taking the lowermost layer to extend from a depth of 2000 km to the base of the mantle (shown by the shaded area in Fig. 2). As expected,  $R$  is largest (2.7) for model *SAW24B16* [3], which has stronger velocity rms than other models in the last 500 km of the mantle (solid line). We obtain  $R = 1.8$  at the bottom of the mantle for both *SB4L18* [4] and *S362D1* [5] (thick dashed line). The uncertainty on  $R$  obtained is relatively large, but the results are compatible with tests we have performed comparing ScS-S and PcP-P residuals in this region. They indicate relatively ‘mild’ values of  $R$  under Eurasia, possibly compatible with a thermal origin of lateral variations in this region (e.g. [24,25]). It is interesting to compare this regional result with that obtained by applying the same methodology to the global dataset. The best variance reduction is obtained for model *SAW24B16* and does not exceed 10% (thin dashed line). In this case, the maximum in variance reduction is much less pronounced, yielding only a lower bound on the value of  $R$  in the bottom layer (always higher than 3). We believe that this reflects the different scales of lateral heterogeneity portrayed by the S models and detected by the PcP-P data, and that the estimate of  $R$  is therefore only meaningful when estimated for well-defined specific regions.

Let us now consider a region well covered by PcP-P, for which smaller scale variations than given in global tomographic models are apparent.

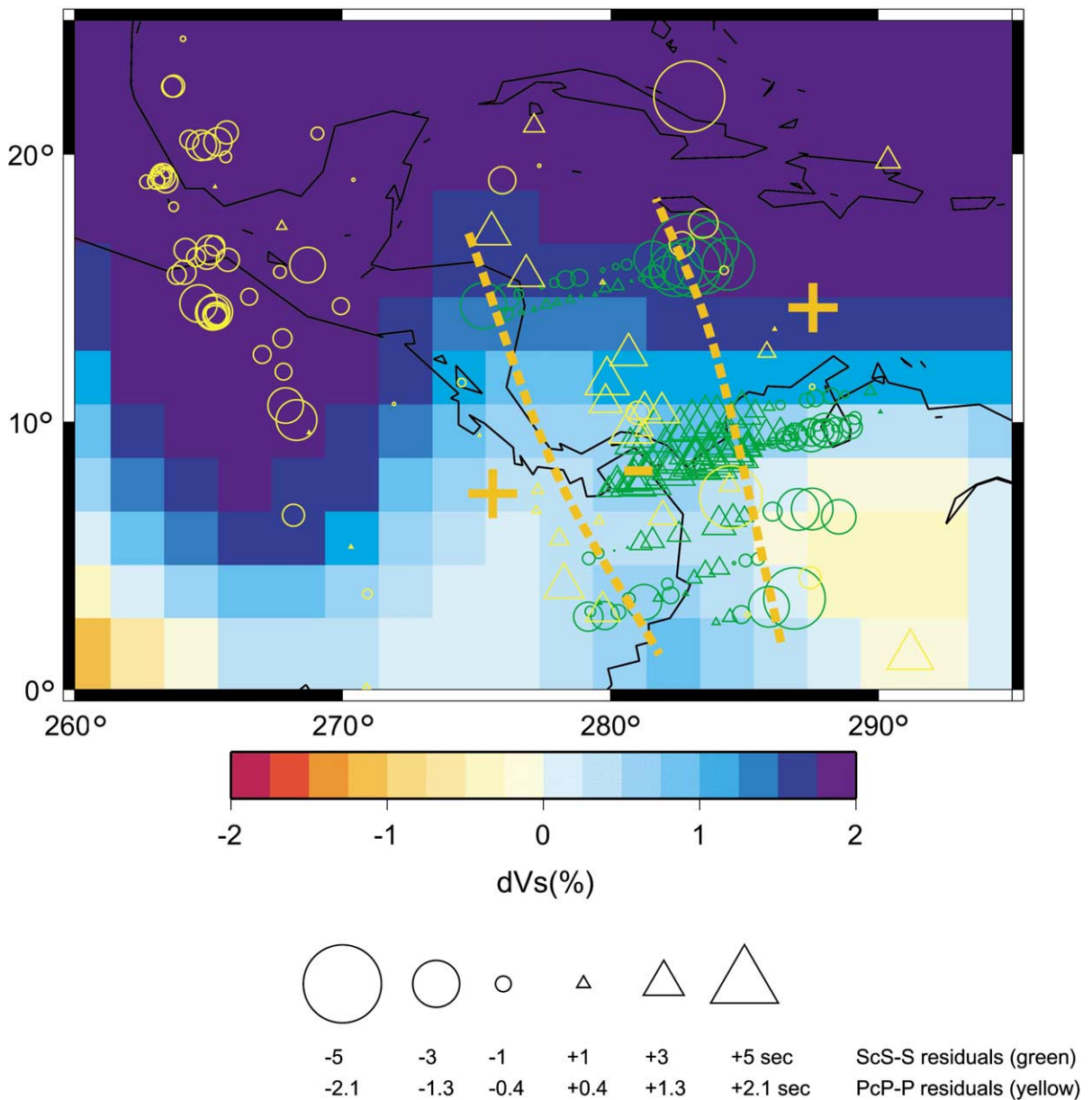


Fig. 3. PcP-P (yellow symbols) and ScS-S (green symbols) travel time residuals plotted at the surface projections of PcP and ScS bouncing points beneath central America. The size of symbols is scaled in such a way that the largest absolute PcP-P residual corresponds to the largest absolute ScS-S residual. The background model is *SAW24B16*. Orange dashed lines delineate the slow velocity anomaly found in the study by Wyssession et al. [10].

One such region is central America. Tomographic models indicate that positive P and S velocity anomalies prevail in the lowermost mantle in this region. In Fig. 3, we plot PcP-P residuals at

the PcP bouncing points (yellow symbols), with model *SAW24B16* in the background. Mostly negative residuals in the northwest of the region are consistent with the tomographic model. How-

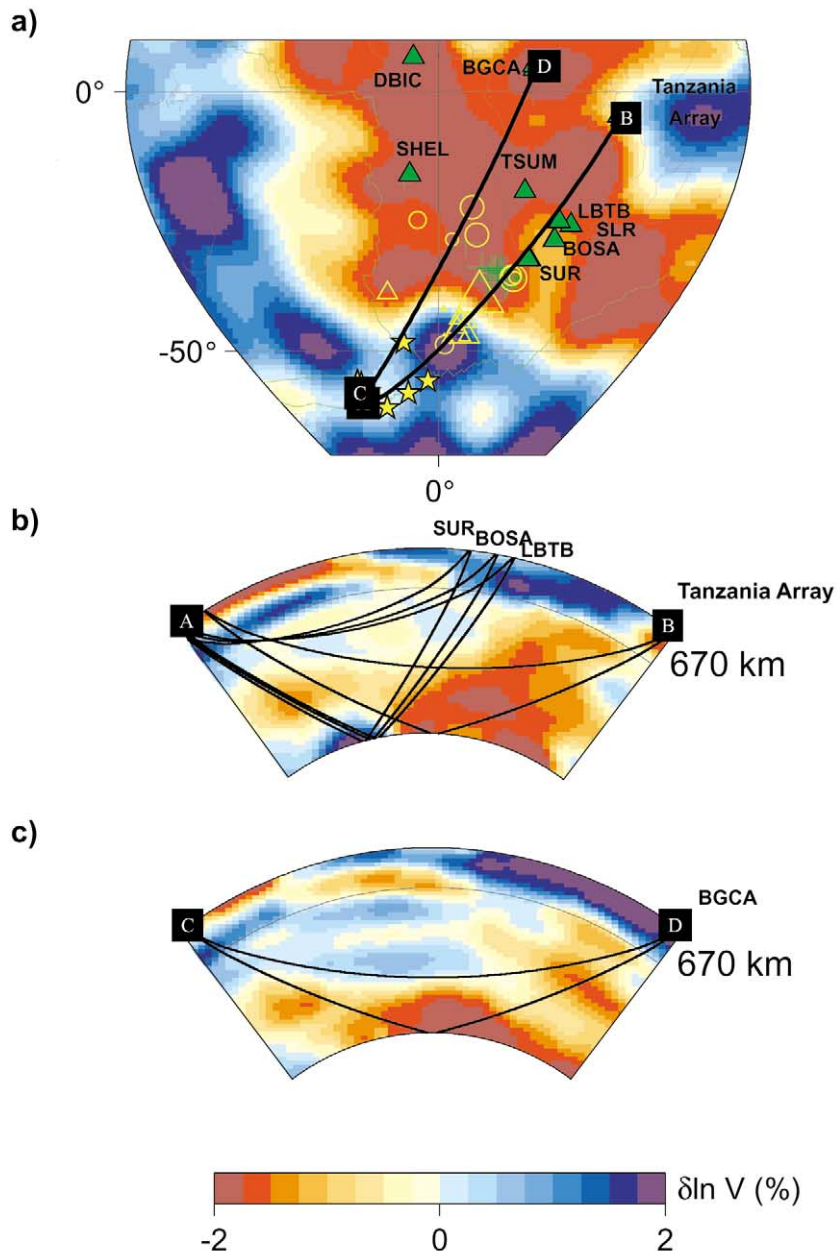


Fig. 4. (a) PcP-P travel time residuals plotted at the surface projections of PcP bouncing points for the south Atlantic/south Africa region. The largest triangle and circle correspond to residuals of +3 s and -1.5 s, respectively. The background model is *SAW24B16*. Green crosses are ScS reflection points. The AB line connects the South Sandwich Island region with the Tanzania network, and the CD line connects the same region with BGCA station. (b) Cross-section through *SAW24B16* along profile AB, with P and PcP paths from a South Sandwich Islands region event to SUR, BOSA and LBTB stations and a south Atlantic ridge event to Tanzania network. (c) Cross-section through *SAW24B16* along profile CD, with P and PcP paths from a South Sandwich Islands region event to BGCA station.

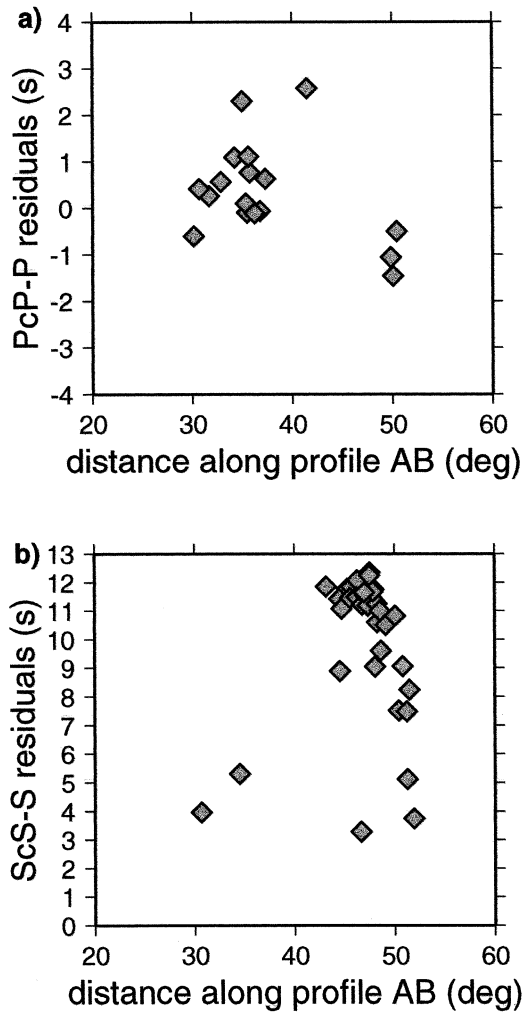


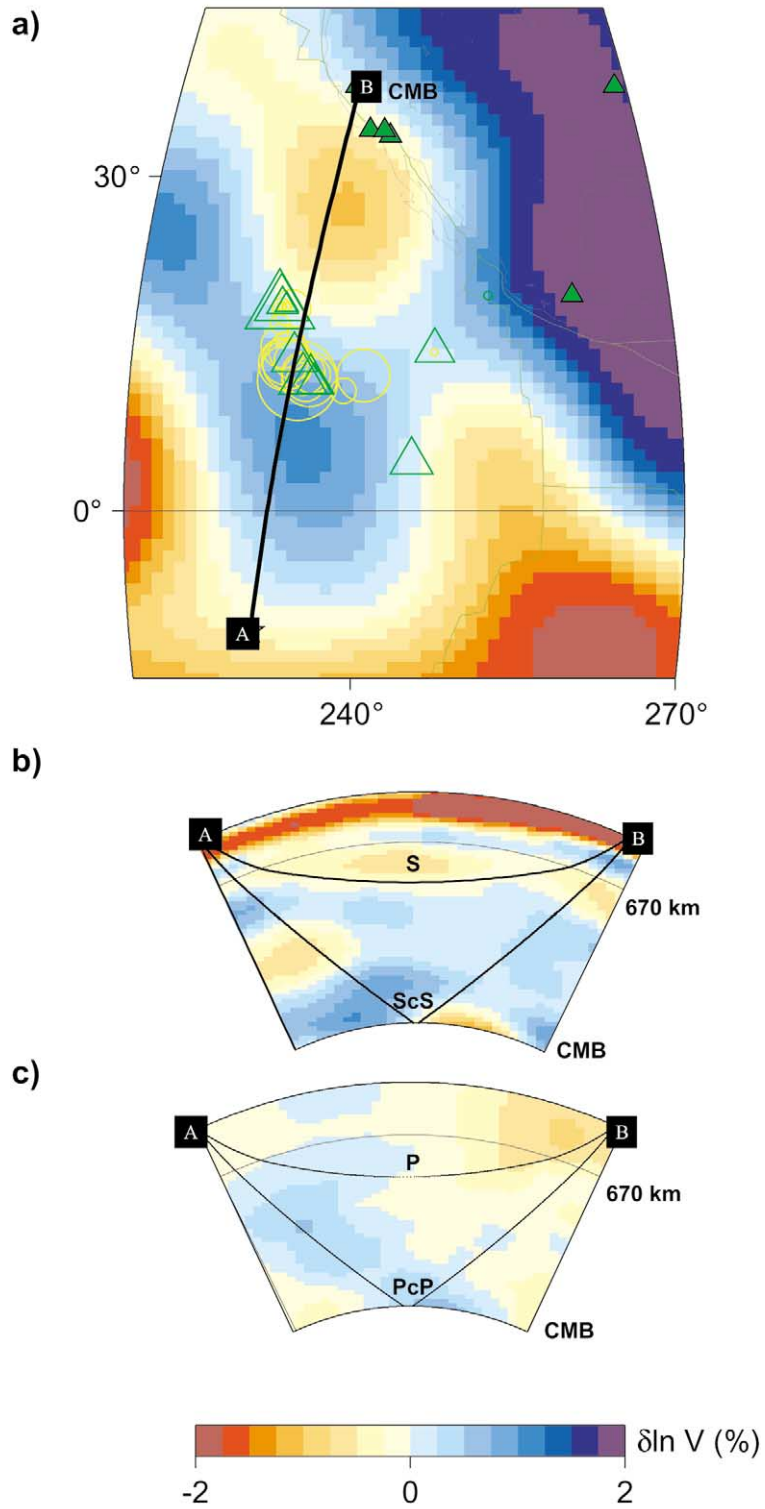
Fig. 5. (a) Subset of PcP-P travel time residuals for paths associated with the AB profile from Fig. 4, plotted as a function of PcP bouncing points distance along the same profile. The residuals are calculated with respect to the *ak135* model, and corrected for ellipticity and the mantle contribution above  $D''$  using the KH2001 model [27]. (b) ScS-S residuals originating from the two events in the south Atlantic: 07/25/94 ( $-56.343$ ,  $-27.395$ ) and 04/14/95 ( $-60.843$ ,  $-20.023$ ), plotted as a function of ScS bouncing points distance along the profile AB. The residuals are calculated with respect to the *PREM* model, and corrected for ellipticity and the *SAW24B16* model above  $D''$ .

ever, PcP-P residuals coherently change from negative to positive and again to mainly negative, when going from southwest to southeast. The range in residuals is on the order of 2 s. This

change occurs on a scale of about  $10^\circ$  at the CMB (i.e.  $\sim 600$  km). For a frequency of  $\sim 1$  Hz, and an epicentral distance of  $\sim 70^\circ$ , the width of the Fresnel zone at the bottom of the mantle is about 480 km (e.g. [26]), which is smaller than the spatial scale of the observed variations. Including mantle path corrections according to the P model of Kárason and van der Hilst [27] does not explain the large PcP-P residuals, nor does it change the size and the sign of the gradient observed. Similarly, Wyssession et al. [10] showed that including mantle path corrections for ScS-S residuals does not change the MOMA cross-array variations in ScS-S residuals. By additional testing, we found that this also holds for models *SAW24B16* and *S362D1*.

In order to compare the variations of PcP-P with ScS-S residuals, we also plotted the ScS-S data of Wyssession et al. [10] in Fig. 3 (without mantle corrections). With only a few exceptions, the variations in PcP-P residuals are in good agreement with the slow (resp. fast) regions delineated by ScS-S. Thus, while the background model only shows a mild northwest–southeast gradient from fast to normal velocities (other S tomographic models give similar results), the differential travel times indicate strong lateral variations on shorter scales, with P velocity tracking S velocity variations. From the range of variations in S and P residuals observed in this region, we infer that  $R$  cannot be much in excess of 2 in  $D''$ , although the sampling is not sufficient to draw completely robust conclusions.

The PcP-P coverage under the Atlantic ocean is very sparse (Fig. 1). However, there is a group of paths from South Sandwich Islands events and a few mid-Atlantic ridge events recorded at various stations in Africa (Fig. 4a). We assembled a total of 22 PcP-P data from 12 events recorded on vertical broadband (20 data) and short period (two data) instruments, in the time period 1980–1998. These data sample  $D''$  near the edge of the southern part of the African superplume, on southwest–northeast oriented paths, as shown in Fig. 4a. PcP-P residuals range from about +3 to  $-1.5$  s along the marked AB profile (Fig. 4a). Fig. 4b shows a vertical cross-section through the line AB, showing three PcP and P paths



from sources in the South Sandwich Islands and stations in south Africa, with model *SAW24B16* in the background. This model shows more complexity than other S tomographic models in the vicinity of our PcP reflection points. It is clear that PcP samples the edge of the African superplume. P tomographic models (not shown) exhibit similar low velocity features on these profiles. The largest negative residual corresponds to a path from the southern mid-Atlantic ridge to station BOSA.

In Fig. 5a, we plot the PcP-P residuals along profile AB as a function of the PcP bottoming point distance from point A. Travel times are corrected for the mantle contribution above *D''* using the KH2001 model, although this does not significantly change the amplitude and the relative variation of residuals (this also holds true when using S velocity models, e.g. *SAW24B16* or *S362D1*). A constant scaling factor from S to P of 0.5 was assumed in the process. Residuals sharply increase between 0° and 10°E, and then go back to negative values at 18°E. Qualitatively, the increase in residuals from west to east out to station LBTB can readily be explained by PcP moving out of the fast velocity region in *D''* and increasingly sampling the low velocities in the plume. The drop to smaller values for the longer path to the Tanzania Array could be partly explained if one allows strong low velocities in the plume to persist high above the CMB, so that both P and PcP are affected. However, absolute travel time measurements for this path indicate that P is delayed by about 1 s and PcP slightly advanced, with respect to *ak135*, so that PcP appears to be detecting fast velocity near the CMB.

Ritsema et al. [7] studied ScS-S and S-SKS travel time residuals along the same path, and also found rapid lateral variations. They proposed a model in which the African plume extends up to 1500 km above the CMB. We measured ScS-S

residuals for the two South Sandwich Island events recorded on the Tanzania Array during its time of operation. The earlier event was already considered in [7]. The measured residuals are shown as crosses at the ScS reflection points in Fig. 4a and range from +1 to +12 s. In Fig. 5b, we plot these residuals as a function of longitude of the ScS reflection point. Even though the sampling is somewhat complementary to that of PcP-P (Fig. 5a), both datasets show similar trends, with a strong increase followed by an abrupt decrease between 0° and 20°E in longitude. The range of variation of P and S residuals is large and occurs on length scales of less than 1000 km, if projected on the CMB. In this region, the sampling is favorable to estimate *R* in the bottom 300–500 km of the mantle from the comparison of ScS-S and PcP-P residuals. We obtain an estimate of  $R = 2.5 \pm 0.3$ , which is not very different from the estimate obtained in Eurasia, although the short scale lateral variations suggest the existence of chemical heterogeneity (e.g. [10]).

Finally, in Fig. 4c, we also consider a slightly more northerly path, CD, on which PcP-P residuals are consistently negative (approx.  $-1.5$  s). This observation is puzzling, because the area of *D''* sampled by PcP is deeper inside the plume, as delineated by tomographic models, and on this profile, the plume does not extend as high above the CMB (Fig. 4c), so that one would expect PcP to be slowed down much more than P. However, we found advanced absolute PcP for these paths. Because these paths correspond to larger epicentral distances (58–72°), even if PcP is affected by structure in the upper mantle, P would be affected in a similar way. We therefore infer that the fast PcP anomaly likely originates at the base of the mantle, in a region where S (and P) velocities are consistently slow in tomographic models. This indicates that lateral variations occur on a shorter scale than seen in tomographic models and possi-

←  
Fig. 6. (a) PcP-P (yellow symbols) and ScS-S (green symbols) travel time residuals plotted at the surface projections of PcP and ScS bouncing points for the eastern Pacific region. The largest triangle and circle correspond to residuals of +9 s and  $-2.2$ s, respectively. The background model is *SAW24B16*. The AB line connects the 94/02/12 event with station CMB in California. (b) Cross-section through *SAW24B16* along profile AB, with the corresponding ScS and S paths. (c) Cross-section through the P model by [28] along profile AB, with the corresponding PcP and P paths.

bly that there are uncorrelated variations in P and S at that scale. Thermal effects alone are unlikely to cause such short scale variations, implying a chemical component to heterogeneity in this region. However, one could also invoke a localized ‘bump’ on the core mantle boundary (with amplitude on the order of 10 km), which is dynamically plausible in a region of upwelling. Unfortunately, the lack of ScS-S data in this specific area prevents us from making more definitive conclusions.

Let us now consider a region of  $D''$ , located in the Pacific, at the eastern edge of the Pacific superplume (Fig. 6a). Our PcP-P dataset consists of 24 measurements from the event of 94/02/12 ( $-10.760$ ,  $-128.857$ ) measured at California stations. We were also able to measure 11 ScS-S differential travel times for the same event. Some stations had usable records for both PcP-P and ScS-S measurements. In this way, we obtained very similar sampling of  $D''$  by PcP and ScS waves. As can be seen from Fig. 6a, the PcP-P residuals are all negative, with a minimum at  $-2.2$  s (with respect to *ak135*), in agreement with predictions of several tomographic P velocity models (e.g. [19,23,28]). On the other hand, all ScS-S residuals with ScS bottoming in the same area are strongly positive, ranging from 3 to 9 s (with respect to *PREM*). There is no systematic variation of residuals with the location. Mantle corrections using KH2001 stripped of  $D''$  shift PcP-P residuals up to 1 s toward zero value, but the corrections for ScS-S from the *SAW24B16* model stripped of  $D''$  do not reduce ScS-S residuals by more than 1 s. The region sampled in the lowermost mantle is not far from the area of study of Bréger and Romanowicz [6] and Bréger et al. [29], who analyzed SKS-Sdiff and ScS-S travel time residuals on paths between Fiji-Tonga and north America. These studies found strong lateral gradients on the eastern border of the Pacific plume, and, in particular, argued for a stronger S velocity contrast (up to +5%) associated with the tongue of fast velocity bordering the plume on the east. The present data sample the eastern side of this ‘tongue’ (see cross-section in Fig. 6b,c) somewhat further south (Fig. 6a). As can be seen from Fig. 6b,c, both ScS and PcP ray paths travel through a thick region of strongly

positive velocity anomaly near the CMB, so that expected PcP-P and ScS-S anomalies are negative. While it is tempting to invoke chemical heterogeneity to explain the negative correlation between P and S velocity anomalies inferred from the PcP-P and ScS-S data, we cannot rule out the possibility that anisotropy at the base of the mantle is a significant factor in affecting PcP and ScS waves in a different way (slowing down ScS or speeding up PcP). Even if the eastern edge of the fast anomaly discussed in [6] is very sharp, it is unlikely that its size and orientation with respect to PcP and ScS ray path geometry would explain such large differences in observed PcP-P and ScS-S anomalies. Interestingly, an anomalously large ratio  $R = \partial \ln V_s / \partial \ln V_p$  was found in a location corresponding to the continuation of this fast P region further toward the west [30]. We suggest that this could be due to a similar situation.

#### 4. Conclusions

We have compared the lateral variations observed in a global dataset of PcP-P differential travel times sensitive to structure in the bottom 500–1000 km of the mantle, to the predictions of global tomographic models, on the one hand, and ScS-S differential travel times, on the other.

This comparison has shown that the different datasets are in good agreement in some regions, in particular in eastern Asia, where fast anomalies over a broad domain are inferred both from tomographic P and S models and from the core-reflected phase data, resulting in a value of  $R$  compatible with a thermal origin of heterogeneity at the base of the mantle in this region. On the other hand, the PcP-P data indicate shorter scale lateral variations in many other regions. We studied in detail two such localized regions, under central America and south-east Africa, which correspond to downwelling and upwelling regions respectively, as seen in global tomographic models. In central America, lateral variations in P and S velocity appear to track each other, and resulting estimates of the ratio  $R$  in the last 500 km of the lower mantle are not particularly high. Under Africa, one profile shows similar results, whereas

a neighboring path to the east indicates fast P velocities in the heart of the low S velocity African ‘plume’. A similar situation is found on the eastern edge of the Pacific plume, where the simultaneous availability of PcP-P and ScS-S data allows us to infer the existence of sharp lateral gradients across compositionally different domains and possibly anisotropy.

Strong lateral variations at the base of the mantle on scale lengths of several hundred kilometers have now been proposed in many studies. Our study documents this further, implying the existence of compositional variations in  $D''$ . We note, however, that the computation of meaningful estimates of  $R$  at the base of the mantle, as an indicator of the nature of heterogeneity, remains a challenge. In order to do it correctly, better spatial sampling in both P and S data is needed, as different smoothing of short scale structures can lead to biased estimates.

In this study, we have mentioned but not assessed quantitatively, the possible influence of anisotropy at the base of the mantle, which could differentially impact PcP and ScS data, and contribute to their apparent incompatibility, in particular in the Pacific, where such anisotropy has been documented (e.g. [31,32]).

Collecting more PcP-P and ScS-S data with a compatible sampling of the lowermost mantle on the one hand, and increasing the resolution and accuracy of tomographic models on the other is necessary to gain further insight regarding the nature of heterogeneity in the lowermost mantle.

## Acknowledgements

Data were obtained from the IRIS Data Management Center. We thank Nicolas Houy, who measured most of the PcP-P travel times used in this study and Michael Wyession for sharing his MOMA S-ScS dataset with us. Figures were made with the General Mapping Tools (P. Wessel and W.H.F. Smith, *EOS Trans. AGU* 76 (1995) 329). We thank Jeroen Ritsema and an anonymous reviewer for helping us improve the manuscript. This is Berkeley Seismological Laboratory contribution 02-08.[AC]

## References

- [1] S.P. Grand, R.D. van der Hilst, S. Widiyantoro, Global seismic tomography: a snapshot of convection in the Earth, *GSA Today* 7 (1997) 1–7.
- [2] J. Ritsema, H.J. van Heijst, J. Woodhouse, Complex shear wave velocity structure imaged beneath Africa and Iceland, *Science* 286 (1999) 1925–1928.
- [3] C. Mégnin, B. Romanowicz, The 3D shear velocity structure of the mantle from the inversion of body, surface, and higher mode waveforms, *Geophys. J. Int.* 143 (2000) 709–728.
- [4] G. Masters, G. Laske, H. Bolton, A.M. Dziewonski, Earth’s Deep Interior: Mineral Physics and Tomography from the Atomic to the Global Scale, in: S.-I. Karato et al. (Eds.), *Geophys. Monogr. Ser.* 117, AGU, Washington, DC, 2000, pp. 63–87.
- [5] Y. Gu, A.M. Dziewonski, Shear velocity of the mantle and discontinuities in the pattern of lateral heterogeneities, *J. Geophys. Res.* 106 (2001) 11169–11199.
- [6] L. Bréger, B. Romanowicz, Three dimensional structure at the base of the mantle beneath the Central Pacific, *Science* 382 (1998) 244–248.
- [7] J. Ritsema, S. Ni, D.V. Helmberger, H.P. Crotwell, Evidence for strong shear velocity reductions and velocity gradients in the lower mantle beneath Africa, *Geophys. Res. Lett.* 25 (1998) 4245–4248.
- [8] S. Ni, D.V. Helmberger, Horizontal transition from fast (slab) to slow (plume) structures at the core-mantle boundary, *Earth. Planet. Sci. Lett.* 187 (2001) 310–310.
- [9] L. Wen, Seismic evidence for a rapidly-varying compositional anomaly at the base of the Earth’s mantle beneath Indian ocean, *Earth Planet. Sci. Lett.* (2001) submitted.
- [10] M.E. Wyession, K.M. Fischer, G.I. Al-eqabi, P.J. Shore, Using MOMA broadband array, ScS-S data to image smaller-scale structures at the base of the mantle, *Geophys. Res. Lett.* 190 (2001) 167–170.
- [11] G.S. Robertson, J.H. Woodhouse, Ratio of relative S to P velocity heterogeneity in the lower mantle, *J. Geophys. Res.* 101 (1996) 20041–20052.
- [12] W. Su, A.M. Dziewonski, Simultaneous inversion for 3-D variations in shear and bulk velocity in the mantle, *Phys. Earth Planet. Int.* 100 (1997) 135–156.
- [13] B.L.N. Kennett, S. Widiyantoro, R.D. van der Hilst, Joint seismic tomography for bulk-sound and shear wave-speed in the Earth’s mantle, *J. Geophys. Res.* 103 (1998) 12469–12493.
- [14] H. Bolton, G. Masters, Travel times of P and S from the global digital seismic networks: implications for the relative variation of P and S velocity in the mantle, *J. Geophys. Res.* 106 (2001) 13527–13540.
- [15] B. Romanowicz, Can we resolve 3D density heterogeneity in the lower mantle?, *Geophys. Res. Lett.* 28 (2001) 1107–1110.
- [16] R.L. Saltzer, R.D. van der Hilst, H. Káráson, Comparing P and S wave heterogeneity in the mantle, *Geophys. Res. Lett.* 28 (2001) 1335–1338.

- [17] E.J. Garnero, D.V. Helmberger, A very slow basal layer underlying large-scale low velocity anomalies in the lower mantle beneath the Pacific: evidence from core phases, *Phys. Earth Planet. Int.* 91 (1995) 161–176.
- [18] J.C. Castle, R.D. van der Hilst, The core-mantle boundary under the Gulf of Alaska: no ULVZ for shear waves, *Earth Planet. Sci. Lett.* 176 (2000) 311–321.
- [19] H. Tkalčić, B. Romanowicz, N. Houy, Constraints on  $D''$  structure using PKP(AB-DF), PKP(BC-DF) and PcP-P travel time data from broadband records, *Geophys. J. Int.* (2001) in press.
- [20] E.R. Engdahl, R.D. van der Hilst, R.P. Buland, Global teleseismic earthquake relocation with improved travel times and procedures for depth determination, *Bull. Seismol. Soc. Am.* 88 (1998) 722–743.
- [21] B.L.N. Kennett, E.R. Engdahl, R. Buland, Constrains on seismic velocities in the Earth from traveltimes, *Geophys. J. Int.* 122 (1995) 108–124.
- [22] A.M. Dziewonski, D.L. Anderson, Preliminary reference Earth model, *Phys. Earth Planet. Int.* 25 (1981) 297–356.
- [23] M. Obayashi, Y. Fukao, P and PcP travel time tomography for the core-mantle boundary, *J. Geophys. Res.* 102 (1997) 17825–17841.
- [24] A. Agnon, M.S.T. Bukowinski,  $\delta_s$  at high pressure and  $\partial \ln V_s / \partial \ln V_p$  in the lower mantle, *Geophys. Res. Lett.* 17 (1990) 1149–1152.
- [25] S. Karato, Importance of anelasticity in the interpretation of seismic tomography, *Geophys. Res. Lett.* 20 (1993) 1623–1626.
- [26] G. Nolet, Seismic wave propagation and seismic tomography, in: G. Nolet (Ed.), *Seismic Tomography*, D. Reidel Publishing Company, Dordrecht, 1987.
- [27] H. Kárason, R.D. van der Hilst, Improving global tomography models of P-wavespeed I: incorporation of differential times for refracted and diffracted core phases (PKP, Pdiff), *J. Geophys. Res.* 106 (2001) 6569–6587.
- [28] L.J. Boschi, A.M. Dziewonski, Whole Earth tomography from delay times of P, PcP, PKP phases: lateral heterogeneities in the outer core, or radial anisotropy in the mantle?, *J. Geophys. Res.* 105 (2000) 13675–13696.
- [29] L. Bréger, B. Romanowicz, C. Ng, The pacific plume as seen by S, ScS, and SKS, *Geophys. Res. Lett.* 28 (2001) 1859–1862.
- [30] H.F. Bolton, Long Period Travel Times and the Structure of the Mantle, PhD Thesis, University of California, San Diego, CA, 1996.
- [31] L. Vinnik, L. Bréger, B. Romanowicz, Anisotropic structures at the base of the Earth's mantle, *Nature* 393 (1998) 255–258.
- [32] S.A. Russell, T. Lay, E.J. Garnero, Seismic evidence for small-scale dynamics in the lowermost mantle at the root of the Hawaiian hotspot, *Nature* 393 (1998) 255–258.